

A MIXTURE-ENERGY-CONSISTENT NUMERICAL APPROXIMATION OF A TWO-PHASE FLOW MODEL FOR FLUIDS WITH INTERFACES AND CAVITATION

MARICA PELANTI

ENSTA ParisTech
Department of Mechanical Engineering
828, Boulevard des Maréchaux
91762 Palaiseau Cedex, France

KEH-MING SHYUE

National Taiwan University
Department of Mathematics
Taipei 106, Taiwan

(Communicated by the associate editor name)

ABSTRACT. We model cavitating flows by a variant of the six-equation single-velocity two-phase model with stiff mechanical relaxation of Saurel–Petitpas–Berry [*J. Comput. Phys.* **228**, 1678 (2009)]. In our approach we employ phasic total energy equations instead of the phasic internal energy equations of the classical system. This alternative formulation allows us to easily design a simple numerical method that ensures consistency with mixture total energy conservation at the discrete level and agreement of the relaxed pressure with the correct mixture equation of state. The two-phase system is solved in two dimensions by a fully-discretized high-resolution wave propagation scheme based on a HLLC/Roe Riemann solver. Numerical experiments show the ability of the numerical model to describe mechanical cavitation processes.

1. Introduction. The modelling of cavitating flows is relevant in numerous areas of engineering, from naval industry to aerospace technology. These flows involve complex thermo-hydrodynamic processes: liquid/vapor phase transition, dynamical creation of interfaces, shock formation. Our ultimate goal is to design new efficient methods for the simulation of cavitating fluids in the framework of diffuse-interface compressible multi-phase flow models [1, 5, 6, 7]. In this work we present the basic numerical model that we have developed, which allows the description of mechanical cavitation processes (with no phase transition). Extensions of this model to account for mass and heat transfer phenomena are reported in [3]. We begin by considering the hyperbolic six-equation single-velocity two-phase flow model with instantaneous pressure relaxation of Saurel–Petitpas–Berry [7], which we recall in Section 2. We propose a variant of this model, by employing phasic total energy equations

2010 *Mathematics Subject Classification.* 65M08,76T10.

Key words and phrases. Compressible two-phase flows, pressure relaxation, cavitation, finite volume schemes, Riemann solvers.

The first author (M. Pelanti) was partially supported by DGA (Direction Générale de l'Armement), Grant DGA 2009.60.035.00.470.75.01. The second author (K.-M. Shyue) was supported in part by the National Science Council of Taiwan Grant NSC 99-2115-M-002-005-MY2.

instead of phasic internal energy equations in the mathematical formulation. This alternative formulation is presented in Section 3, and the numerical scheme used for the system solution is described in Section 4. The mixture-energy-consistency property of the numerical method is discussed in Section 4.1. Some numerical experiments are finally illustrated in Section 5.

2. The six-equation single-velocity two-phase flow model. The single-velocity two-phase flow model with stiff mechanical relaxation of Saurel *et al.* [7] (see also [8]) in one spatial dimension has the form

$$\partial_t \alpha_1 + u \partial_x \alpha_1 = \mu(p_1 - p_2), \quad (1a)$$

$$\partial_t(\alpha_1 \rho_1) + \partial_x(\alpha_1 \rho_1 u) = 0, \quad (1b)$$

$$\partial_t(\alpha_2 \rho_2) + \partial_x(\alpha_2 \rho_2 u) = 0, \quad (1c)$$

$$\partial_t(\rho u) + \partial_x(\rho u^2 + \alpha_1 p_1 + \alpha_2 p_2) = 0, \quad (1d)$$

$$\partial_t(\alpha_1 \mathcal{E}_1) + \partial_x(\alpha_1 \mathcal{E}_1 u) + \alpha_1 p_1 \partial_x u = -p_I \mu(p_1 - p_2), \quad (1e)$$

$$\partial_t(\alpha_2 \mathcal{E}_2) + \partial_x(\alpha_2 \mathcal{E}_2 u) + \alpha_2 p_2 \partial_x u = p_I \mu(p_1 - p_2). \quad (1f)$$

Here α_k is the volume fraction of phase k , $k = 1, 2$, ρ_k is the phasic density, p_k the phasic pressure, and \mathcal{E}_k the phasic internal energy, $\mathcal{E}_k = \rho_k \varepsilon_k$, where ε_k denotes the phasic specific internal energy. Moreover, $\rho = \alpha_1 \rho_1 + \alpha_2 \rho_2$ is the mixture density and u denotes the flow velocity. The source terms appearing in the volume fraction equation and in the phasic energy equations model mechanical relaxation. In these terms μ is the pressure relaxation parameter and p_I the interface pressure, $p_I = \frac{Z_2 p_1 + Z_1 p_2}{Z_1 + Z_2}$, where $Z_k = \rho_k c_k^2$ is the acoustic impedance of phase k , and c_k is the phasic sound speed. As in [7, 8], the pressure relaxation parameter μ is assumed to be infinite, that is we consider instantaneous mechanical equilibrium. The closure of system (1) is obtained through the specification of equations of state for the two phases, which we express here in terms of \mathcal{E}_k and ρ_k , $p_k = p_k(\mathcal{E}_k, \rho_k)$, $k = 1, 2$. The phasic sound speed can be written as $c_k = \sqrt{\kappa_k h_k + \chi_k}$, where $h_k = \frac{\mathcal{E}_k + p_k}{\rho_k}$ is the phasic specific enthalpy, $\kappa_k = \frac{\partial p_k(\mathcal{E}_k, \rho_k)}{\partial \mathcal{E}_k}$ and $\chi_k = \frac{\partial p_k(\mathcal{E}_k, \rho_k)}{\partial \rho_k}$. The mixture sound speed is $c = \sqrt{Y_1 c_1^2 + Y_2 c_2^2}$, where $Y_k = \frac{\alpha_k \rho_k}{\rho}$ is the mass fraction of phase k . Here we will restrict our study to the case of species governed by the stiffened gas law (SG EOS), $p_k = (\gamma_k - 1)\mathcal{E}_k - \gamma_k \pi_k - (\gamma_k - 1)\eta_k \rho_k$, where γ_k , π_k , η_k are constant parameters. The mixture specific internal energy is defined as $\varepsilon = Y_1 \varepsilon_1 + Y_2 \varepsilon_2$, and, equivalently, the mixture energy $\mathcal{E} = \rho \varepsilon$ is $\mathcal{E} = \alpha_1 \mathcal{E}_1 + \alpha_2 \mathcal{E}_2$. This relation, by using $\mathcal{E}_k = \mathcal{E}_k(p_k, \rho_k)$ with $p_1 = p_2 = p$, determines the equation of state for the mixture pressure $p = p(\mathcal{E}, \rho_1, \rho_2, \alpha_1)$. In the particular case of the SG EOS we obtain

$$p(\mathcal{E}, \rho_1, \rho_2, \alpha_1) = \left(\mathcal{E} - (\alpha_1 \rho_1 \eta_1 + \alpha_2 \rho_2 \eta_2) - \left(\frac{\alpha_1 \gamma_1 \pi_1}{\gamma_1 - 1} + \frac{\alpha_2 \gamma_2 \pi_2}{\gamma_2 - 1} \right) \right) / \left(\frac{\alpha_1}{\gamma_1 - 1} + \frac{\alpha_2}{\gamma_2 - 1} \right). \quad (2)$$

Let us finally remark that the model (1) is hyperbolic and it has eigenvalues given by $\lambda_1 = u - c$, $\lambda_2 = \lambda_3 = \lambda_4 = \lambda_5 = u$, $\lambda_6 = u + c$.

3. Phasic-total-energy-based formulation. For numerical reasons that we will discuss in the following, we propose to consider a mathematically equivalent formulation of the model (1), obtained by replacing the two phasic internal energy equations with two phasic total energy equations. We denote with E_k the total

energy of phase k , $E_k = \mathcal{E}_k + \frac{1}{2}\rho_k u^2$. The two-phase model (1) then takes the form

$$\partial_t \alpha_1 + u \partial_x \alpha_1 = \mu(p_1 - p_2), \quad (3a)$$

$$\partial_t(\alpha_1 \rho_1) + \partial_x(\alpha_1 \rho_1 u) = 0, \quad (3b)$$

$$\partial_t(\alpha_2 \rho_2) + \partial_x(\alpha_2 \rho_2 u) = 0, \quad (3c)$$

$$\partial_t(\rho u) + \partial_x(\rho u^2 + \alpha_1 p_1 + \alpha_2 p_2) = 0, \quad (3d)$$

$$\partial_t(\alpha_1 E_1) + \partial_x(u \alpha_1 (E_1 + p_1)) + \Sigma(q, \partial_x q) = -p_1 \mu(p_1 - p_2), \quad (3e)$$

$$\partial_t(\alpha_2 E_2) + \partial_x(u \alpha_2 (E_2 + p_2)) - \Sigma(q, \partial_x q) = p_1 \mu(p_1 - p_2), \quad (3f)$$

where the non-conservative contribution Σ in the phasic total energy equations is

$$\begin{aligned} \Sigma(q, \partial_x q) &= -u((Y_2 p_1 + Y_1 p_2) \partial_x \alpha_1 + \alpha_1 Y_2 \partial_x p_1 - \alpha_2 Y_1 \partial_x p_2) \\ &= -u(Y_2 \partial_x(\alpha_1 p_1) - Y_1 \partial_x(\alpha_2 p_2)), \end{aligned} \quad (3g)$$

and where we have denoted with q the vector of the system unknowns. The sum of the phasic energy equations (3e) and (3f) recovers the equation expressing conservation of the mixture total energy $E = \mathcal{E} + \rho \frac{u^2}{2} = \alpha_1 E_1 + \alpha_2 E_2$:

$$\partial_t E + \partial_x(u(E + \alpha_1 p_1 + \alpha_2 p_2)) = 0. \quad (4)$$

In compact form the system reads:

$$\partial_t q + \partial_x f(q) + \sigma(q, \partial_x q) = \psi(q), \quad \text{with} \quad (5a)$$

$$q = \begin{pmatrix} \alpha_1 \\ \alpha_1 \rho_1 \\ \alpha_2 \rho_2 \\ \rho u \\ \alpha_1 E_1 \\ \alpha_2 E_2 \end{pmatrix}, \quad f = \begin{pmatrix} 0 \\ \alpha_1 \rho_1 u \\ \alpha_2 \rho_2 u \\ \rho u^2 + \alpha_1 p_1 + \alpha_2 p_2 \\ u \alpha_1 (E_1 + p_1) \\ u \alpha_2 (E_2 + p_2) \end{pmatrix}, \quad \sigma = \begin{pmatrix} u \partial_x \alpha_1 \\ 0 \\ 0 \\ 0 \\ \Sigma \\ -\Sigma \end{pmatrix}, \quad \psi = \begin{pmatrix} \mu(p_1 - p_2) \\ 0 \\ 0 \\ 0 \\ -p_1 \mu(p_1 - p_2) \\ p_1 \mu(p_1 - p_2) \end{pmatrix}. \quad (5b)$$

Above, we have put into evidence the conservative portion of the system $\partial_x f(q)$, where $f(q)$ is the flux function, and the non-conservative term $\sigma(q, \partial_x q)$. The source term $\psi(q)$ contains the pressure relaxation terms.

4. Numerical method. To numerically solve system (5) we use a fractional step technique, similar to [7, 8], where we alternate between the solution of the homogeneous hyperbolic system and the solution of a system of ordinary differential equations (ODEs) that takes into account pressure relaxation source terms. The second step drives the two-phase flow to mechanical equilibrium.

The steps of the algorithm are the following:

1. *Homogeneous hyperbolic system.* We solve over a time interval Δt the homogeneous hyperbolic portion of (5):

$$\partial_t q + \partial_x f(q) + \sigma(q, \partial_x q) = 0. \quad (6)$$

2. *Pressure relaxation.* We solve in the limit $\mu \rightarrow \infty$ the system of ordinary differential equations (ODEs)

$$\partial_t q = \psi(q). \quad (7)$$

This step relaxes the phasic pressures to an equilibrium value $p_1 = p_2 = p$ (*relaxed pressure*). In this step the partial densities, the mixture momentum, the mixture total energy and the mixture internal energy remain constant.

The volume fraction α_1 , the mixture pressure p and the phasic energies $\alpha_k \mathcal{E}_k$, $\mathcal{E}_k = \mathcal{E}_k(p, (\alpha_k \rho_k)/\alpha_k)$ are updated before returning to Step 1.

4.1. Mixture-energy-consistent discretization. Let us denote with superscript 0 the quantities computed by solving the homogeneous system in Step 1 of the algorithm above, and with superscript * the quantities at mechanical equilibrium computed in Step 2. Let us also denote with $E^{0,C}$ discrete values of the mixture total energy that come from a conservative approximation of the conservation law for E in (4).

Definition 4.1. We say that the numerical scheme based on the fractional step algorithm above is *mixture-energy-consistent* if the following two properties are satisfied

(i) *Mixture total energy conservation consistency:*

$$E^0 = E^{0,C}, \quad \text{where} \quad E^0 = (\alpha_1 E_1)^0 + (\alpha_2 E_2)^0. \quad (8a)$$

(ii) *Relaxed pressure consistency:*

$$\mathcal{E}^{0,C} = \alpha_1^* \mathcal{E}_1(p^*, \frac{(\alpha_1 \rho_1)^0}{\alpha_1^*}) + \alpha_2^* \mathcal{E}_2(p^*, \frac{(\alpha_2 \rho_2)^0}{\alpha_2^*}), \quad \text{where} \quad \mathcal{E}^{0,C} = E^{0,C} - \frac{((\rho u)^0)^2}{2\rho^0}. \quad (8b)$$

The first property (i) means that the sum of the discrete values of the phasic total energies given by the solution of the homogeneous system must recover discrete values of the mixture total energy that are consistent with a conservative discrete form of (4). The second property (ii) means that the value of the relaxed (equilibrium) pressure p^* predicted in the relaxation step must be equal to the pressure as computed through the mixture equation of state $p(\mathcal{E}^{0,C}, \alpha_1^*, \rho_1^*, \rho_2^*)$. In the particular case of the SG EOS this consistency condition reads

$$p^* = \left(\mathcal{E}^{0,C} - ((\alpha_1 \rho_1)^0 \eta_1 + (\alpha_2 \rho_2)^0 \eta_2) - \left(\frac{\alpha_1^* \gamma_1 \pi_1}{\gamma_1 - 1} + \frac{\alpha_2^* \gamma_2 \pi_2}{\gamma_2 - 1} \right) \right) / \left(\frac{\alpha_1^*}{\gamma_1 - 1} + \frac{\alpha_2^*}{\gamma_2 - 1} \right). \quad (9)$$

The mathematical formulation of the two-phase model with the phasic total energy equations (3) easily allows us to satisfy both properties (i) and (ii). To ensure property (i), it suffices in Step 1 to apply a standard conservative scheme to the conservative portion of the energy equations $\partial_t(\alpha_k E_k) + \partial_x(u \alpha_k (E_k + p_k))$, $k = 1, 2$, and to discretize symmetrically the non-conservative contribution Σ written in (3g). In such a way the sum of the discrete non-conservative energy equations recovers a conservative discrete form of the mixture energy equation, as a consequence of the cancellation of non-conservative discrete contributions. The fulfillment of mixture total energy conservation consistency then easily enables us to ensure also property (ii), the agreement of the relaxed equilibrium pressure with the correct mixture equation of state. See the simple pressure relaxation procedure for Step 2 in Section 4.3. On the other hand, it appears difficult to obtain a mixture-energy-consistent scheme if we apply an analogous fractional step algorithm to the classical 6-equation two-phase model (1). Although clearly both formulations (1) and (3) mathematically recover the conservation law for the mixture total energy, it is hard to discretize the phasic internal energies equations (1e) and (1f) in a way that recovers a conservative discrete form of (4). Indeed, numerical models such as [7, 8] built on the formulation (1) need to augment the 6-equation system with the equation for E . The additional conservation law for E is solved through a standard conservative scheme to obtain consistent discrete values $E^{0,C}$. These values are then used to correct the thermodynamic state predicted by the non-conservative

internal energy equations. Note that this approach in general does not guarantee the consistency property (ii), $p^* = p(\mathcal{E}^{0,C}, \alpha_1^*, \rho_1^*, \rho_2^*)$.

4.2. Solution of the homogeneous system. To solve the homogeneous system (6) we employ the wave propagation algorithms of [2], which are a class of Godunov-type finite volume methods to approximate hyperbolic systems of partial differential equations. Assuming a uniform grid with cells of width Δx , and denoting with Q_i^n the approximate solution of q at the i th cell and at time t^n , the updating formula of the second-order one-dimensional scheme has the form

$$Q_i^{n+1} = Q_i^n - \frac{\Delta t}{\Delta x} (\mathcal{A}^+ \Delta Q_{i-1/2} + \mathcal{A}^- \Delta Q_{i+1/2}) - \frac{\Delta t}{\Delta x} (F_{i+1/2}^h - F_{i-1/2}^h), \quad (10)$$

where $\mathcal{A}_{i+1/2}^\mp \Delta Q$ are the so-called *fluctuations* at interfaces $x_{i+1/2}$ between cells i and $(i+1)$, and $F_{i+1/2}^h$ are correction fluxes for second order resolution. The fluctuations $\mathcal{A}_{i+1/2}^\mp \Delta Q$ are computed by solving Riemann problems at cells interfaces for each pair of data Q_i^n, Q_{i+1}^n . A Riemann solver must be supplied to perform this task. We have developed two approximate Riemann solvers for the model system (5): a HLLC solver, similar to the solvers described in [7, 8], and a new Roe solver [4]. Both solvers can be easily designed to ensure mixture-energy-consistency (Def. 4.1), see [3] for details. The expression of the Roe eigenstructure for the Roe method is reported in Appendix A. The HLLC method, as expected, is more robust than the Roe method, and it is the method that we choose to employ for the one-dimensional scheme and for the computation of normal waves in the two-dimensional scheme. The Roe eigenstructure is useful in the two-dimensional wave propagation algorithm to define transverse fluctuations [2]. This is done by projecting the normal fluctuations obtained via the HLLC solver onto the basis of Roe eigenvectors associated to the orthogonal direction.

4.3. Pressure relaxation step. We consider Step 2 of the fractional step algorithm (solution of (7)), which drives the system to mechanical equilibrium. We employ a procedure similar to the relaxation technique illustrated in [7]. We will use here the superscript notation introduced in Section 4.1. We easily see that the solution of the system of equations (7) gives $(\alpha_k \rho_k)^* = (\alpha_k \rho_k)^0$, $k = 1, 2$, $(\rho u)^* = (\rho u)^0$, $E^* = E^0$, $\mathcal{E}^* = \mathcal{E}^0$. By assuming a linear variation of the interface pressure p_I with α_1 , by integration we obtain the two equations:

$$(\alpha_k E_k)^* - (\alpha_k E_k)^0 = (\alpha_k \mathcal{E}_k)^* - (\alpha_k \mathcal{E}_k)^0 = (-1)^k \frac{p_I^0 + p_I^*}{2} (\alpha_1^* - \alpha_1^0), \quad k = 1, 2. \quad (11)$$

At the final time we impose mechanical equilibrium: $p_1^* = p_2^* = p_I^* = p^*$. Then, by using the phasic equations of state $\mathcal{E}_k = \mathcal{E}_k(p_k, \rho_k)$, the two equations above give the solution for the equilibrium values α_1^* and p^* . For the particular case of the SG EOS we obtain a simple quadratic equation for the relaxed pressure p^* (which has always a physically admissible solution). Let us now remark that the values α_1^* and p^* by construction satisfy $\mathcal{E}^0 = \alpha_1^* \mathcal{E}_1(p^*, \frac{(\alpha_1 \rho_1)^0}{\alpha_1^*}) + \alpha_2^* \mathcal{E}_2(p^*, \frac{(\alpha_2 \rho_2)^0}{\alpha_2^*})$. Since the wave propagation scheme that we employ in Step 1 recovers conservation-consistent discrete values of the mixture total energy from the computed phasic energies, $E^0 = (\alpha_1 E_1)^0 + (\alpha_2 E_2)^0 = E^{0,C}$, then we deduce that the simple pressure relaxation procedure described here computes the thermodynamically correct value of the equilibrium pressure p^* . Both properties (i) and (ii) of Definition 4.1 are ensured, and therefore the numerical scheme is mixture-energy-consistent.

5. Numerical experiments.

5.1. 1D cavitation tube. We perform the one-dimensional cavitation tube test proposed in [7] (see also [5]). We consider a tube filled with liquid water at atmospheric pressure, $p = 10^5$ Pa. The liquid ($\rho_l = 1000$ kg/m³) contains initially a uniformly distributed small amount of air ($\alpha_g = 10^{-2}$, $\rho_g = 1$ kg/m³). The SG EOS parameters are $\gamma_l = 4.4$, $\pi_l = 6 \times 10^8$ Pa, $\eta_l = 0$ J/kg for the liquid, and $\gamma_g = 1.4$, $\pi_g = 0$ Pa, $\eta_g = 0$ J/kg for air. A velocity discontinuity is set at the middle of the tube at initial time, with $u = -100$ m/s on the left and $u = 100$ m/s on the right. Two strong rarefactions symmetrically propagating in opposite directions are generated, which induce a decrease of the liquid pressure in the middle region of the tube. In this region the gas volume fraction increases, generating a cavitation pocket (mechanical cavitation). Second-order results at time $t = 1.85$ ms obtained with the HLLC solver (and MC limiter) with 1000 grid cells are shown in Figure 1 (CFL = 0.5). They are in good agreement with those reported in [7]. We have also tested the Roe solver for this experiment and results are not distinguishable from those obtained with the HLLC solver.

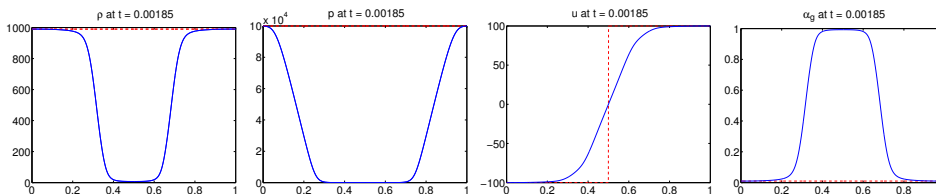


FIGURE 1. Cavitation tube test. From left to right: mixture density, mixture pressure, velocity, gas volume fraction.

5.2. Cavitating Richtmyer–Meshkov instability. We consider the cavitating water-gas Richtmyer–Meshkov instability test problem proposed in [7]. A curved interface (with left-facing convexity) at initial time separates a region filled with nearly pure water ($\alpha_g = 10^{-6}$) and a region of nearly pure gas ($\alpha_l = 10^{-6}$). The initial pressure is $p = 10^5$ Pa, and the densities $\rho_l = 1000$ kg/m³ and $\rho_g = 100$ kg/m³. Both water and gas have an initial velocity of -200 m/s. The SG EOS parameters are those used in [7]. Top, bottom and left boundaries are solid walls, whereas the right side is a free flow boundary. When the flow impinges against the left wall a right-going shock wave propagates through the curved water-gas interface generating a Richtmyer–Meshkov instability. The pressure decrease in the expansion zones close to the left wall generates cavitation pockets in this region. Second-order results obtained with the HLLC solver and Roe transverse splitting are displayed in Figure 2 (grid with 600×200 cells, CFL = 0.5), and they qualitatively agree with those reported in [7].

5.3. High-velocity underwater projectile. We perform the high-velocity underwater projectile numerical experiment presented in [6] (see also [5]). Liquid water at speed $u = 600$ m/s flows over an immersed obstacle with hexagonal section. Initially the liquid is at atmospheric pressure, $p = 10^5$ Pa, and it has density $\rho_l = 1500$ kg/m³. A small amount of vapor is present in the liquid at initial time, $\alpha_g = 10^{-3}$. The SG EOS for the two phases are those used in [6]. Due to the symmetry of the problem, we carry the computation only on the portion of the physical domain above the symmetry axis. We use a uniform grid with 600×200 cells

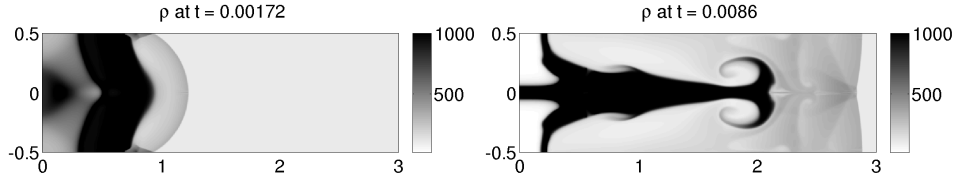


FIGURE 2. Cavitating Richtmyer–Meshkov instability experiment. Density at $t = 1.72$ and $t = 8.6$ ms.

over a rectangular computational domain that is mapped to a curvilinear grid in the physical domain. The flow interaction with the edges of the obstacle generates strong rarefaction waves, which determine a pressure decrease and consequently the growth of a cavitation wake. After a time sufficiently large the flow reaches a configuration with a stationary cavitation zone. Second-order numerical results obtained with the HLLC solver are shown in Figure 3 (CFL = 0.5).

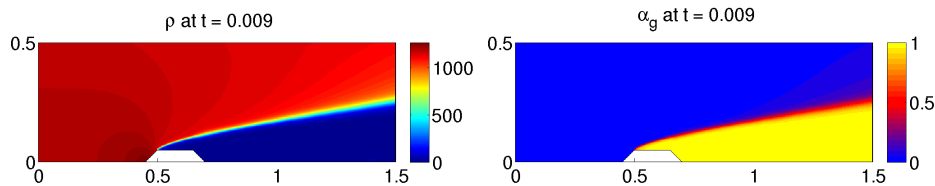


FIGURE 3. High-speed underwater projectile experiment. Density and gas volume fraction at $t = 0.9$ s (approximately stationary conditions).

6. Conclusions. We have developed a new numerical model for two-phase compressible flows based on the single-velocity 6-equation two-phase flow model with stiff pressure relaxation of Saurel *et al.* [7]. We have proposed a variant of the standard model system [7, 8] that easily allows us to design a mixture-energy-consistent numerical scheme, in contrast with the classical formulation. A fully-discretized two-dimensional high-resolution wave propagation scheme has been developed for the system solution. We have already developed an extended numerical model that includes thermal and chemical potential relaxation source terms to describe heat and mass transfer processes. This is illustrated in [3].

Appendix A. Roe matrix and eigenstructure. We consider the quasi-linear form of system (6), $\partial_t q + A(q)\partial_x q = 0$, and following the classical Roe approach [4], we define an approximate solver by using the exact solution to the Riemann problem for a linearized system $\partial_t q + \tilde{A}(q_\ell, q_r)\partial_x q = 0$ with initial left and right data q_ℓ and q_r . The definition of the Roe matrix $\tilde{A}(q_\ell, q_r)$ must guarantee conservation of the partial densities $\alpha_k \rho_k$, $k = 1, 2$, the mixture momentum ρu , and the mixture total energy E . That is, denoting with $q^{(l)}$ the l th component of q , and with $f^{(l)}$ the associated flux function (l th component of $f(q)$), the Roe matrix \tilde{A} must be defined such that $\sum_{j=1}^6 \tilde{A}_{lj}(q_r - q_\ell)^{(j)} = f^{(l)}(q_r) - f^{(l)}(q_\ell)$, $l = 2, 3, 4$, and $\sum_{j=1}^6 (\tilde{A}_{5j} + \tilde{A}_{6j})(q_r - q_\ell)^{(j)} = f_E(q_r) - f_E(q_\ell)$, where \tilde{A}_{lj} is the entry (l, j) of the matrix \tilde{A} , and $f_E = u(E + \alpha_1 p_1 + \alpha_2 p_2)$ is the flux function for the mixture total

energy E , see equation (4). Following again [4], the Roe matrix \tilde{A} is defined as the matrix $A(q)$ of the original system evaluated in an average state $\tilde{q} = \tilde{q}(q_\ell, q_r)$. By imposing the conservation conditions above, a Roe matrix for the model system (6) closed with the SG EOS can be determined as $\tilde{A} = A(\hat{u}, \hat{Y}_1, \widehat{uY_1}, \widehat{Y_1H_1}, \widehat{Y_2H_2})$, where the averaged quantities \hat{u} , \hat{Y}_1 , \hat{Y}_2 , $\widehat{uY_1}$, $\widehat{uY_2}$, $\widehat{Y_1H_1}$, $\widehat{Y_2H_2}$ are defined as

$$\hat{u} = \frac{u_\ell \sqrt{\rho_\ell} + u_r \sqrt{\rho_r}}{\sqrt{\rho_\ell} + \sqrt{\rho_r}}, \quad \hat{Y}_k = \frac{Y_{k\ell} \sqrt{\rho_\ell} + Y_{kr} \sqrt{\rho_r}}{\sqrt{\rho_\ell} + \sqrt{\rho_r}}, \quad (12a)$$

$$\widehat{uY_k} = \frac{(uY_k)_\ell \sqrt{\rho_\ell} + (uY_k)_r \sqrt{\rho_r}}{\sqrt{\rho_\ell} + \sqrt{\rho_r}}, \quad \widehat{uY_k} = \frac{1}{2} (\hat{u} \hat{Y}_k + \widehat{uY_k}), \quad (12b)$$

$$\widehat{Y_kH_k} = \frac{(Y_kH_k)_\ell \sqrt{\rho_\ell} + (Y_kH_k)_r \sqrt{\rho_r}}{\sqrt{\rho_\ell} + \sqrt{\rho_r}}, \quad k = 1, 2. \quad (12c)$$

Note that $\hat{Y}_1 + \hat{Y}_2 = 1$ and $\widehat{uY_1} + \widehat{uY_2} = \hat{u}$. The Roe eigenvalues are given by

$$\tilde{\lambda}_1 = \hat{u} - \tilde{c}, \quad \tilde{\lambda}_2 = \tilde{\lambda}_3 = \tilde{\lambda}_4 = \tilde{\lambda}_5 = \hat{u}, \quad \tilde{\lambda}_6 = \hat{u} + \tilde{c}, \quad (13)$$

where $\tilde{c} = \sqrt{\widehat{Y_1c_1^2} + \widehat{Y_2c_2^2}}$ with $\widehat{Y_kc_k^2} = \kappa_k (\widehat{Y_kH_k} - \frac{\hat{u}^2}{2} \hat{Y}_k) + \chi_k \hat{Y}_k$.

The corresponding matrix of the Roe right eigenvectors, $\tilde{R} = [\tilde{r}_1, \dots, \tilde{r}_6]$, is

$$\tilde{R} = \begin{pmatrix} 0 & 0 & 0 & 0 & 1 & 0 \\ \hat{Y}_1 & 0 & 0 & 1 & 0 & \hat{Y}_1 \\ \hat{Y}_2 & 0 & 1 & 0 & 0 & \hat{Y}_2 \\ \hat{u} - \tilde{c} & 0 & \hat{u} & \hat{u} & 0 & \hat{u} + \tilde{c} \\ \widehat{Y_1H_1} - \widehat{uY_1} \tilde{c} & -\frac{\kappa_2}{\kappa_1} & -\frac{\chi_2}{\kappa_1} + \frac{\kappa_2}{\kappa_1} \frac{\hat{u}^2}{2} & -\frac{\chi_1}{\kappa_1} + \frac{\hat{u}^2}{2} & \frac{\Pi_1 - \Pi_2}{\kappa_1} & \widehat{Y_1H_1} + \widehat{uY_1} \tilde{c} \\ \widehat{Y_2H_2} - \widehat{uY_2} \tilde{c} & 1 & 0 & 0 & 0 & \widehat{Y_2H_2} + \widehat{uY_2} \tilde{c} \end{pmatrix}. \quad (14)$$

Above $H_k = h_k + \frac{u^2}{2}$, $\kappa_k = (\gamma_k - 1)$, $\chi_k = -(\gamma_k - 1)\eta_k$ and $\Pi_k = \gamma_k \pi_k$, $k = 1, 2$.

REFERENCES

- [1] A. K. Kapila, R. Menikoff, J. B. Bdzil, S. F. Son and D. S. Stewart, *Two-phase modeling of deflagration-to-detonation transition in granular materials: Reduced equations*, Physics of Fluids, **13** (2001), 3002–3024.
- [2] R. J. LeVeque, “Finite Volume Methods for Hyperbolic Problems”, Cambridge University Press, 2002.
- [3] M. Pelanti and K.-M. Shyue, *A mixture-energy-consistent six-equation two-phase numerical model for fluids with interfaces, cavitation and evaporation waves*, submitted.
- [4] P. L. Roe, *Approximate Riemann solvers, parameter vectors, and difference schemes*, J. Comput. Phys., **43** (1981), 357–372.
- [5] R. Saurel and O. Le Métayer, *A multiphase model for compressible flows with interfaces, shocks, detonation waves and cavitation*, J. Fluid Mech., **431** (2001), 239–271.
- [6] R. Saurel, F. Petitpas and R. Abgrall, *Modelling phase transition in metastable liquids: application to cavitating and flashing flows*, J. Fluid Mech., **607** (2008), 313–350.
- [7] R. Saurel, F. Petitpas and R. A. Berry, *Simple and efficient relaxation methods for interfaces separating compressible fluids, cavitating flows and shocks in multiphase mixture*, J. Comput. Phys., **228** (2009), 1678–1712.
- [8] A. Zein, M. Hantke and G. Warnecke, *Modeling phase transition for compressible two-phase flows applied to metastable liquids*, J. Comput. Phys., **229** (2010), 2964–2998.

Received xxxx 20xx; revised xxxx 20xx.

E-mail address: marica.pelanti@ensta-paristech.fr

E-mail address: shyue@ntu.edu.tw